

ON-CHIP INTERNALIZATION PROCESS OF AN INTRACELLULAR NANOBOT INTO A SINGLE CELL

K. Ogawa¹, K. Uesugi¹, and K. Morishima¹

¹Osaka University, Suita, JAPAN

ABSTRACT

This paper reports on-chip internalization of an intracellular nanobot into a single cell with a microfluidic device. The nanobot was made of a Ni sputtered carbon nanocoil and driven by a rotating magnetic field. Here, we fabricated the microfluidic device to capture a single cell by a soft lithography technique and demonstrated on-chip internalization of the nanobot. As a result, a single cell was captured in the microfluidic device and the nanobot was successfully internalized into the trapped cell. Additionally the nanobot could be driven at a speed of 0.35 $\mu\text{m/s}$ inside the cell. This result indicates the potential of the nanobot which can move to any positions inside a single cell for intracellular stimulation.

INTRODUCTION

In the biomedical field, the target of the research has been transferred to a cell which is a minimum unit of living things. Inside cells, different organelles exist and determine cell's vitality. For example, mitochondria control the production of ATP and apoptosis. It is expected that artificial control of its functions will be the new method of healing cancer or other disease. Accordingly, the functions and method of controlling them have been investigated. Recently, it has been reported that organelles are stimulated chemically, electrically and mechanically from the outside of cells to control its functions. Deutsch's group stimulated cardiomyocytes electrically and measured intracellular fluorescein fluorescence polarization [1]. Nakamura's group applied electric stimulus and mechanical tension to cardiomyocytes by an electro-tensile bioreactor [2]. Although all organelles are affected by such methods, unrelated organelles are also affected simultaneously. In addition, these kinds of stimuli way damage to cells.

In order to stimulate only the specific organelle, it is essential to directly stimulate from cell-interior. It is important to control the stimulating position precisely inside cells for intracellular stimulation. Therefore nanobots are required. At micro or nanoscales such as inside cells, one of the most important factors is achieving efficient energy supply. Since it is difficult for a nanobot to be equipped with a battery because of its scale, the energy needs to be supplied by the wireless. For example, researchers have developed catalytic nanobots that exhibit autonomous propulsion and perform various advanced function [3,4]. While chemically driven nanobots have received enormous attention, the elimination of external fuel is required for important applications such as biomedical ones. In order to respond this need, biocompatible propulsion mechanisms without external fuel have been investigated recently. For example, Wang's group developed artificial nanomachines which displayed efficient propulsion in the presence of either magnetic and acoustic fields without adding any chemical fuel [5,6].

However, few papers have reported the biomedical application of nanobots such as stimulation of cells or organelles.

For this reason, we have adopted carbon nanocoils (CNCs) with Ni layer as nanobots to control the function of organelle (Figure 1a) [7,8]. The nanobot has a helical shape and can demonstrate corkscrew motion like flagella, whose motion is well suited to the low-Raynolds-number environment such as the inside of cells [9], by a rotating magnetic field. In previous work, we succeeded in internalizing nanobots into cells. However, the nanobots had difficulties to be internalized into a specific cell. In addition, it is difficult to observe some reactions of stimulated cells because reagents for analysis cannot be exchanged on a culture dish. In this paper, we proposed on-chip internalization of the nanobot into a single cell with a microfluidic device (Figure 1b). By using the microfluidic device, it becomes possible to separate a single cell from many cells and analyze some local biochemical reactions. Here, we designed and fabricated the microfluidic device. Then we demonstrated internalization of the nanobot into a single cell with the microfluidic device.

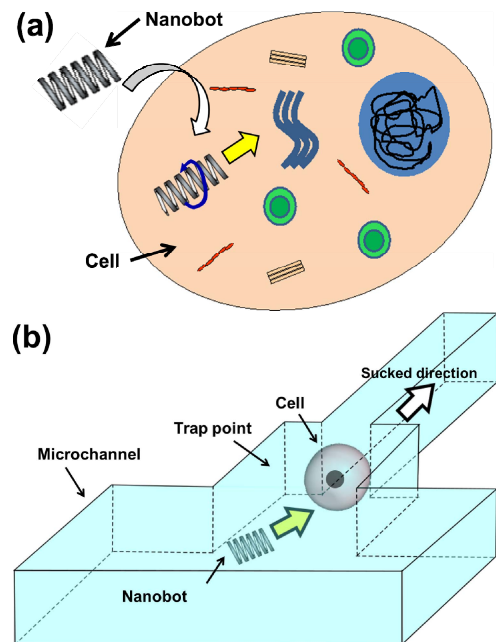


Figure 1: (a) Concept of an intracellular nanobot for stimulating organelles. (b) Principle of on-chip internalization of the nanobot into a single cell. A single cell is captured at the trap point. Then, the nanobot is approached to the cell by a rotating magnetic field.

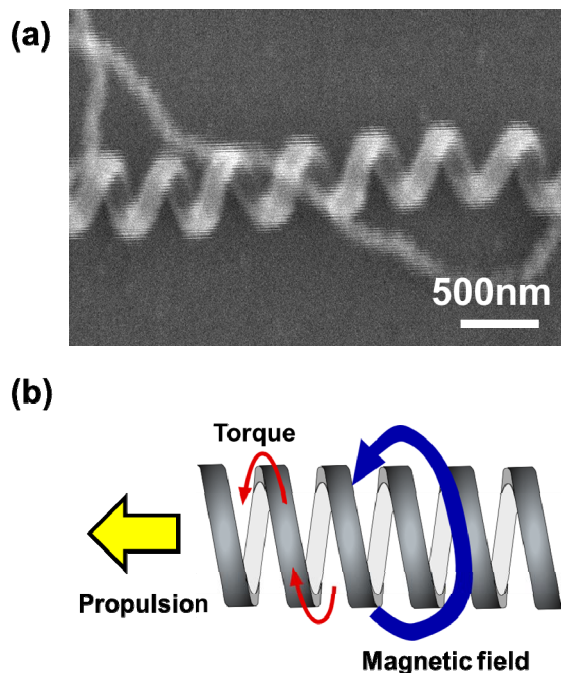


Figure 2: (a) SEM image of an intracellular nanobot with Ni layer of 80 nm. (b) Driving principle of nanobots. The rotating magnetic field is generated by three orthogonal Helmholtz coil pairs.

EXPERIMENTAL

Magnetically driven nanobots

CNCs were prepared by chemical vapor deposition using a catalyst of Fe-In-Sn-O [10]. The average of the tube, diameter and pitch forming CNCs used in this paper was 153 nm, 520 nm and 323 nm. In order to add a magnetic property to CNCs, Ni layer was sputtered on the surface of CNCs by sputtering device (Shibaura CFS-4ES-SS). A scanning electron microscope (SEM) image of a nanobot with Ni layer of 80 nm is shown in Figure 2a.

The nanobots can be driven due to the helical shape and deviation of formed magnetic material under a rotating magnetic field. The constant magnetic field aligns magnetized the nanobots parallel to the direction of the applied magnetic field. This makes it possible to rotate the nanobots by turning the applied constant magnetic field (Figure 2b). Three orthogonal Helmholtz coil pairs which can create a uniform magnetic field between them were used to generate a rotating magnetic field. The magnetic intensity and rotating frequency were operated by a controller. The Helmholtz coil pairs were put on an inverted microscope stage (Nikon Ti-U).

Design and fabrication of the microfluidic device

The microfluidic device to separate a single cell from many cells was fabricated from polydimethylsiloxane (PDMS) by a soft lithography technique (Figure 3). The device was composed of an inlet channel, outlet channel and trap channel. Although cells can move through the inlet and outlet channels (width, 100 μm), the cells cannot pass through the trap channel (width, 3 μm). Therefore,

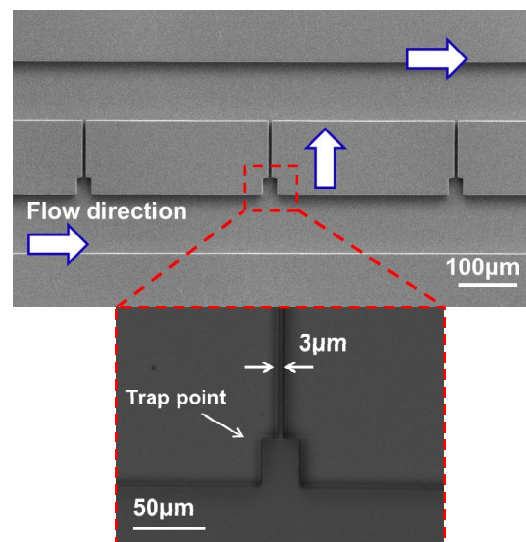


Figure 3: SEM and microscopic images of the microfluidic device

cells can be trapped at the trap point (width, 30 μm ; length, 25 μm). First, the SU-8 photoresist was spin-coated onto a silicon wafer to obtain a 20- μm -thickness master. PDMS prepolymer was poured onto the silicon master and baked at 100 $^{\circ}\text{C}$ for 1 h. Then the solid polymer was peeled off and punched for an inlet and outlet. The PDMS structure was bonded to the surface of cover slip.

Cell culture

C2C12 cells (Riken Cell Bank), which the method of culture and observation has been already established, were prepared for the investigation. The cells were maintained at 37 $^{\circ}\text{C}$ with a 5% CO_2 atmosphere in Dulbecco's Modified Eagle's Medium (DMEM, Wako Pure Chemical Industries), which was supplemented with 10 % fetal bovine serum (Invitrogen), 100 units/mL penicillin, and 100 $\mu\text{g}/\text{mL}$ streptomycin (Sigma-Aldrich).

Preparation for internalization process

The microfluidic device was placed on the inverted microscopy stage. C2C12 cells stained with CellTracker Red (Thermo Fisher Scientific) were removed from a culture dish by adding 0.25 % trypsin-EDTA solution (Sigma-Aldrich). The suspension of C2C12 cells was pipetted into the inlet and the gentle suction was applied to the outlet at a 1 $\mu\text{L}/\text{min}$ flow rate using a syringe pump (ISIS CX07200). After the cells were captured at the trap point, the nanobots coated with Lipofectamine 2000 transfection reagent (Invitrogen) were pipetted into the inlet. The nanobots were modified with FITC-BSA (Thermo Fisher Scientific) for fluorescent observation [11]. Briefly, CNCs were suspended in a concentrated $\text{H}_2\text{SO}_4/\text{HNO}_3$ mixture (3:1 v/v) and sonicated for 3 h. The suspension was centrifuged, washed with distilled water several time and dried. FITC-BSA and CNCs were then incubated at 4 $^{\circ}\text{C}$ overnight and free FITC-BSA was removed. The density of cells and nanobots which were pipetted into the inlet was 1000 cells/ μL and 1 $\mu\text{g}/\mu\text{L}$, respectively.

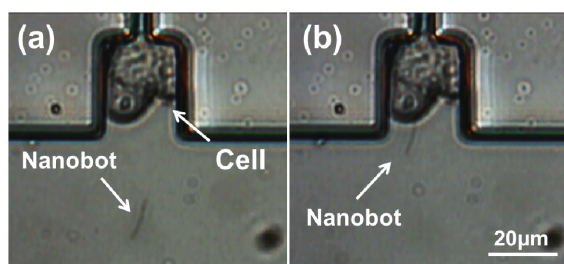


Figure 4: Microscopic images of internalization process. (a) The cell was captured at the trap point and the nanobot was introduced into the microfluidic device. (b) The nanobot was approached and attached to the trapped cell by applying a rotating magnetic field.

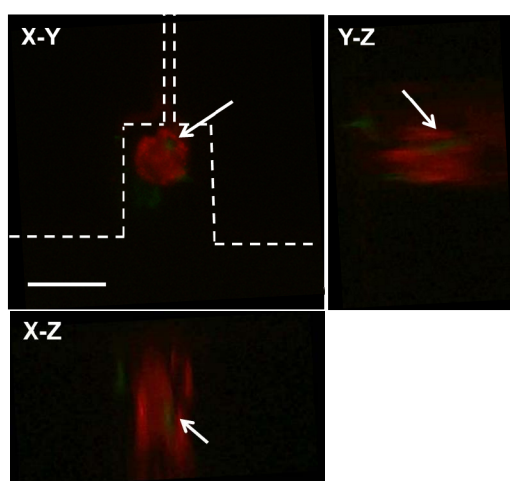


Figure 5: Fluorescence microscopic images of the trapped cell after incubating. The red and green (arrowed) parts indicated cytoplasm and the nanobot, respectively. Scale bar: 20 μm .

RESULT AND DISCUSSION

On-chip internalization of nanobots

Figure 4 indicated the internalization process of the nanobot. A single cell was captured at the trap point in the microfluidic device because it was partly sucked. After stopping the flow, the nanobot which was pipetted into the microfluidic device (Figure 4a) was approached to the trapped cell by applying a rotating magnetic field and attached to the cell (Figure 4b). After incubating for 6 h, the nanobot was internalized into the trapped cell (Figure 5). The green and red parts showed the nanobot and cytoplasm, respectively. Due to X-Z and Y-Z sections, the green part was contained in the red part. This indicated that the nanobot was internalized into the targeted cell. Moreover, using such a device lead to internalize the nanobots into some targeted cells at the same time. The survival rate of cells with nanobots was more than 90 %. Accordingly, to internalize the nanobots had little cytotoxicity. In general, nickel displays cytotoxicity. The weight of nickel which was sputtered on the surface of

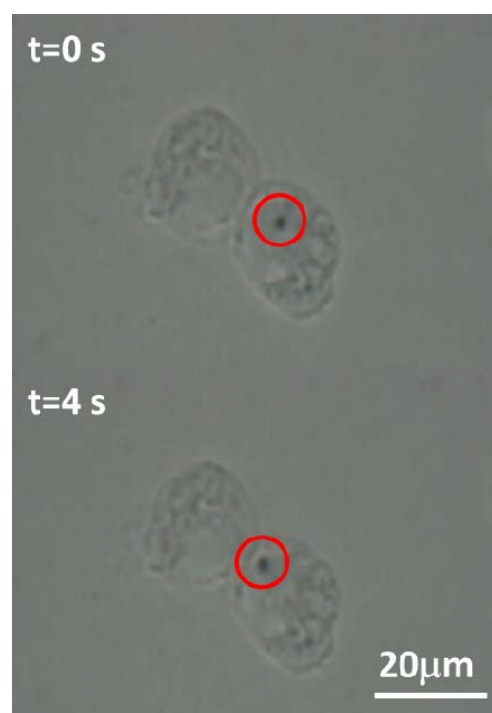


Figure 6: Microscopic image of the motion of the nanobot inside a cell (circled in red).

nanobots was approximately 3.6×10^{-13} g. The low cytotoxicity of nanobots is considered to be due to small quantity of nickel [12].

The nanobot was internalized by lipofection because it was coated with transfection reagent. The internalization efficiency of the nanobots was approximately 20 %. This value was lower than that in case of DNA transfection [13]. The size of contained vesicles was tens of nanometer because the reagent was generally used for DNA transfection. However, the size of nanobots was one hundred times as large as that of DNA and some nanobots were not covered with the vesicles. Therefore, it will be required to contain the nanobots with giant vesicles [14] to improve the internalization efficiency.

Demonstration of driving nanobots inside cells

The cells which the nanobots were internalized were removed from the microfluidic device and seeded on a culture dish. Cells have few spaces and high viscosity in their bodies. Therefore, it is difficult for nanobots to drive inside cells. Here, in order to drive nanobots inside cells, the change of osmotic pressure was applied. Cells with nanobots were filled with Dulbecco's Phosphate-Buffered Saline (DPBS, Wako Pure Chemical Industries) diluted by 100 times with pure water and the intracellular solution got hypotonic by difference in osmotic pressure. In this condition, cells became expanded and the viscosity got smaller. The survival rate of cells in the solution was approximately 70 %.

By applying a rotating magnetic field, the nanobot could be driven inside a cell (Figure 6). The velocity of the nanobot inside a cell was $0.35 \mu\text{m/s}$, using a magnetic rotational frequency of 5 Hz. The velocity was one eighth

as low as that of the nanobots driven in water. Because of the difference in osmotic pressure, convective flow occurred inside a cell and disturbed the motion of the nanobot. Therefore, we will attempt to have the driving force of nanobots larger by improving the magnetic field generating device. Additionally, it is assumed that the nanobots will be used as carriers for organelle-targeted drug delivery because some drugs or chemicals could be modified on CNCs like carbon nanotubes [15].

CONCLUSION

The main contribution of this paper was to develop on-chip internalization process of nanobots and drive them inside cells. In order to achieve on-chip internalization, we fabricated the microfluidic device to capture a single cell and succeeded in internalizing the nanobot into the cell. Moreover, the nanobot was driven inside a cell at a speed of 0.35 $\mu\text{m/s}$.

This result suggests the possibility to control on-chip internalization of the intracellular nanobot. Various kinds of chemicals and biomolecules could be modified on its surface. It could be a promising method for driving inside a cell and stimulating organelles of a single cell. In the future, the demonstrated capabilities should enable fundamental changes in the concept of medical diagnosis and treatment.

ACKNOWLEDGEMENTS

This work was financially supported by JSPS KAKENHI Grant Numbers Nos. 15H00819, 26249027, 21676002, 23111705.

REFERENCES

- [1] D. Fixler, R. Tirosh, T. Zinman, A. Shainberg, M. Deutsch, "Fluorescence polarization: A novel indicator of cardiomyocyte contraction," *Biochemical and Biophysical Research Communications*, vol. 300, pp. 23-28, 2003.
- [2] Z. Feng, T. Matsumoto, Y. Nomura, T. Nakamura, "An electro-tensile bioreactor for 3-D culturing of cardiomyocytes," *IEEE Engineering in Medicine and Biology Magazine*, vol. 24, pp. 73-79, 2005.
- [3] Z. Wu, Y. Wu, W. He, X. Lin, J. Sun, Q. He, "Self-propelled polymer-based multilayer nanorockets for transportation and drug release," *Angewandte Chemie International Edition*, vol. 52, no. 27, pp. 7000-7003, 2013.
- [4] A. A. Solovev, W. Xi, D. H. Gracias, S. M. Harazim, C. Deneke, S. Sanchez, O. G. Schmidt, "Self-Propelled Nanotools," *ACS Nano*, vol. 6, pp. 1751-1756, 2012.
- [5] V. Garcia-Gradilla, J. Orozco, S. Sattayasamitsathit, F. Soto, F. Kuralay, A. Pourazary, A. Katzenberg, W. Gao, Y. Shen, J. Wang, "Functionalized ultrasound-propelled magnetically guided nanomotors: Toward practical biomedical applications," *ACS Nano*, vol. 7, pp. 9232-9240, 2013.
- [6] J. Li, T. Li, T. Xu, M. Kiristi, W. Liu, Z. Wu, J. Wang, "Magneto-Acoustic Hybrid Nanomotor," *Nano Letter*, vol. 15, pp. 4814-4821, 2015.
- [7] T. Matsumoto, T. Hoshino, Y. Akiyama, K. Morishima, "A novel application of carbon nano coils for intracellular nano-robots," in *Proceedings of 2011 IEEE 6th International Conference on NEMS*, 2011, pp. 1089-1092.
- [8] K. Ogawa, O. Suekane, K. Morishima, "Carbon nano magnetic coil machine driving inside a cell," *Proceedings of 2015 19th International Conference on μTAS* , 2015, pp. 2110-2111.
- [9] D. J. Bell, S. Leutenegger, K. M. Hammar, L. X. Dong, B. J. Nelson, "Flagella-like propulsion for microrobots using a nanocoil and a rotating electromagnetic field," in *IEEE 23th International Conference on ICRA 2007*, 2007, pp. 1128-1133.
- [10] S. Yang, X. Chen, S. Motojima, M. Ichihara, "Morphology and microstructure of spring-like carbon micro-coils/nano-coils prepared by catalytic pyrolysis of acetylene using Fe-containing alloy catalysts," *Carbon*, vol. 43, no. 4, pp. 827-834, 2005.
- [11] Q. Mu, G. Du, T. Chen, B. Zhang, B. Yan, "Suppression of human bone morphogenetic protein signaling by carboxylated single-walled carbon nanotubes," *ACS Nano*, vol. 3, no. 5, pp. 1139-1144, 2009.
- [12] H. Yin, H. P. Too, G. M. Chow, "The effects of particle size and surface coating on the cytotoxicity of nickel ferrite," *Biomaterials*, vol. 26, no. 29, pp. 5818-5826, 2005.
- [13] Y. Wang, Q. W. Lin, P. P. Zheng, J. S. Zhang, F. R. Huang, "DHA inhibits protein degradation more efficiently than EPA by regulating the PPAR γ /NF κ B pathway in C2C12 myotubes," *Biomed Research International*, vol. 2013, 2013.
- [14] Y. Natsume T. Toyota, "Giant Vesicles Containing Microspheres with High Volume Fraction Prepared by Water-in-oil Emulsion Centrifugation," *Chemistry Letters*, vol. 42, no. 3, pp. 295-297, 2013.
- [15] N. W. S. Kam, M. O'Connell, J. a Wisdom, H. Dai, "Carbon nanotubes as multifunctional biological transporters and near-infrared agents for selective cancer cell destruction," *Proceedings of National Academy of Sciences of the United States of America*, vol. 102, no. 33, pp. 11600-11605, 2005.

CONTACT

*K. Morishima, tel: +81-6-6879-7343;

E-mail: morishima@mech.eng.osaka-u.ac.jp

Web: <http://www-live.mech.eng.osaka-u.ac.jp/>